The Root Foraging Response under Low Nitrogen Depends on *DWARF1*-Mediated Brassinosteroid Biosynthesis[1][OPEN]

Zhongtao Jia, Ricardo F.H. Giehl, and Nicolaus von Wirén[2,3]

Molecular Plant Nutrition, Department of Physiology and Cell Biology, Leibniz Institute of Plant Genetics and Crop Plant Research, 06466 Gatersleben, Germany

ORCID IDs: 0000-0003-0233-1578 (Z.J.); 0000-0003-1006-3163 (R.F.H.G.); 0000-0002-4966-425X (N.v.W.).

Root developmental plasticity enables plants to adapt to limiting or fluctuating nutrient conditions in the soil. When grown under nitrogen (N) deficiency, plants develop a more exploratory root system by increasing primary and lateral root length. However, mechanisms underlying this so-called foraging response remain poorly understood. We performed a genome-wide association study in Arabidopsis (*Arabidopsis thaliana*) and we show here that noncoding variations of the brassinosteroid (BR) biosynthesis gene *DWARF1* (*DWF1*) lead to variation of the *DWF1* transcript level that contributes to natural variation of root elongation under low N. In addition to *DWF1*, other central BR biosynthesis genes upregulated under low N include *CONSTITUTIVE PHOTOMORPHOGENIC DWARF*, *DWF4*, and *BRASSINOSTEROID-6-OXIDASE2*. Phenotypic characterization of knockout and knockdown mutants of these genes showed significant reduction of their root elongation response to low N, suggesting a systemic stimulation of BR biosynthesis to promote root elongation. Moreover, we show that low N-induced root elongation is associated with aboveground N content and that overexpression of *DWF1* significantly improves plant growth and overall N accumulation. Our study reveals that mild N deficiency induces key genes in BR biosynthesis and that natural variation in BR synthesis contributes to the root foraging response, complementing the impact of enhanced BR signaling observed recently. Furthermore, these results suggest a considerable potential of BR biosynthesis to genetically engineer plants with improved N uptake.

Optimal growth and development of plants depend largely on their ability to cope with adverse or unfavorable environmental conditions. With regard to nutrient availability, plant roots are often exposed to spatial heterogeneity and temporal fluctuations of nutrient concentrations in the soil solution. To ensure adequate nutrient uptake, plants must continuously integrate external nutrient availability with their internal nutrient demand to "decide" upon the induction of physiological adaptations, such as the release of nutrient-mobilizing exudates (Badri and Vivanco, 2009; Schmid et al., 2014) and the expression of nutrient transporters at the root plasma membrane (Yuan et al., 2007; Wang et al., 2012a), or upon morphological adaptations that modulate root system architecture (Giehl and von Wirén, 2014). Responses of the root system to changing or inadequate nutrient availability can be positive or negative. Suppressed root proliferation is frequently the consequence of prolonged periods of nutrient starvation when decreasing investment into growth processes coincides with depletion of internal nutrient pools (Gruber et al., 2013; Kellermeier et al., 2014). Nonetheless, even under severe nutrient deficiency, root proliferation appears to be primarily regulated by signaling mechanisms before growth processes become completely exhausted (Pérez-Torres et al., 2008; Krouk et al., 2010; Araya et al., 2014). On the other hand, suppressed root proliferation may result from elevated or toxic concentrations of mineral elements in the substrate. Primary roots exhibit a particularly high sensitivity to elevated levels of certain minerals, including aluminum, ammonium, and iron (Kochian et al., 2015; Liu and von Wirén, 2017; Abel, 2017). Root system architectural changes can also be triggered by complex signaling mechanisms such as phosphorus deficiency-induced iron excess, which damages the apical root meristem via callose formation (Müller et al., 2015).

Positive growth responses of the root system to low or localized nutrient supplies are commonly described as foraging responses. These responses are expressed in enhanced proliferation of the whole root system, particularly in response to mild deficiencies of nitrogen (N) or phosphorus (Pérez-Torres et al., 2008; Gruber et al., 2013), or in lateral roots exploring local patches with

[1]This work was supported by the China Scholarship Council (CSC; grant no. 201406350062 to Z.J.).

[2]Author for contact: vonwiren@ipk-gatersleben.

[3]Senior author.

The author responsible for distribution of materials integral to the findings presented in this article in accordance with the policy described in the Instructions for Authors (www.plantphysiol.org) is: Nicolaus von Wirén (vonwiren@ipk-gatersleben).

Z.J. performed experiments; R.F.H.G. supervised qPCR analyses; Z.J., R.F.H.G., and N.v.W. designed experiments, analyzed the data, and wrote the article; and N.v.W. supervised the project.

[OPEN]Articles can be viewed without a subscription.

www.plantphysiol.org/cgi/doi/10.1104/pp.20.00440

elevated supplies of nitrate (Drew, 1975; Remans et al., 2006), phosphate (Drew, 1975), iron (Giehl et al., 2012), or ammonium (Lima et al., 2010). Nitrogen has a particularly strong impact on root system architecture, as roots respond not only to the level and distribution of N but also to the forms of N present in the external environment (Giehl and von Wirén, 2014; Forde, 2014; Liu and von Wirén, 2017; Jia and von Wirén, 2020). The ground-breaking work of Drew (1975) showed that plants can stimulate lateral root proliferation into N-rich patches where adequate amounts of nitrate or ammonium are available. More recent work has demonstrated that these two N forms act synergistically to regulate root system architecture, as localized ammonium provokes higher-order lateral root branching (Lima et al., 2010) while nitrate primarily stimulates lateral root elongation (Zhang and Forde, 1998; Remans et al., 2006; Guan et al., 2014; Liu et al., 2020). In the case of nitrate-driven lateral root elongation, underlying signaling pathways have been identified in which the nitrate transceptor NITRATE TRANSPORTER1.1 (NRT1.1) plays a dual role. In the absence of nitrate, NRT1.1 facilitates shootward auxin movement to prevent lateral root outgrowth (Krouk et al., 2010; Bouguyon et al., 2015), whereas in the presence of nitrate, NRT1.1 activates a downstream signaling cascade involving the MADS-box transcription factor *ARABIDOPSIS NITRATE REGULATED1* (*ANR1*) to stimulate lateral root elongation (Remans et al., 2006; Mounier et al., 2014). Analogous to nitrate, the high-affinity AMMONIUM TRANSPORTER1;3 (AMT1;3) takes in a key function by driving lateral root branching in response to localized ammonium supply (Lima et al., 2010). Whether this response is also hormone regulated remains to be investigated.

Root development under varied N availability shows a strict dose-dependent regulation that can be subdivided into three scenarios (Giehl and von Wirén, 2014). Ample supply of N, and specifically of nitrate, induces a systemic N signal to repress root growth, which involves the auxin signaling modules *miR167/ARF8* and *miR393/AFB3* (Gifford et al., 2008; Vidal et al., 2010). When exposed to severe N limitation, plant roots adopt a "survival strategy" and completely restrict the formation of new lateral roots. This response is triggered by the removal of auxin from lateral root tips via the auxin transport function of NRT1.1 and the CLAVATA3/ESR-related (CLE)-CLAVATA1 signaling module that arrests lateral root development under severe N limitation (Krouk et al., 2010; Araya et al., 2014). When roots are subjected to decreasing N availability that causes mild N deficiency, lateral root emergence increases moderately, whereas elongation of primary and lateral roots is strongly induced (Gruber et al., 2013; Ma et al., 2014). These architectural modifications result in a systemic foraging response that increases soil exploration by an expanded root system (Giehl and von Wirén, 2014) but at the cost of a lower root diameter and lower cell wall stability (Qin et al., 2019). Although TRP AMINOTRANSFERASE RELATED2 (TAR2)-mediated auxin biosynthesis is critical for lateral root emergence under mild N deficiency, lateral root elongation is largely independent of TAR2 (Ma et al., 2014). Instead, brassinosteroids (BRs) are involved, as natural allelic variation in BRASSINOSTEROID SIGNALING KINASE3 (BSK3) can contribute up to 12% of the primary root elongation under mild N deficiency (Jia et al., 2019). Thus, further regulatory mechanisms must exist that contribute to the root foraging response under low N (LN).

Here, we further explore a genome-wide association (GWA) approach in Arabidopsis (*Arabidopsis thaliana*) to uncover genes involved in root foraging under mild N deficiency. We identify *DWARF1* (*DWF1*), a key gene involved in BR biosynthesis, as a further molecular determinant for root elongation in response to LN. Moreover, we show that in addition to *DWF1*, mild N deficiency also upregulates the expression of other central BR biosynthesis genes, a crucial step in promoting root elongation under this condition. Thus, our study uncovers that the root foraging response observed under mild N deficiency relies on a systemic upregulation of BR biosynthesis in roots, complementing the recently observed enhanced sensitivity of the BR signaling pathway.

RESULTS

Natural Variation of Root Length Traits in Two N Environments

Our previous study of the Arabidopsis ecotype Col-0 showed that total lateral root length and total root length exhibited a pronounced increase under moderate or mild N deficiency (Gruber et al., 2013). To identify the genetic components modulating root growth under LN, we measured total lateral root length as well as total root length in a diverse panel of 200 Arabidopsis accessions in a GWA study (Supplemental Table S1). At both N environments, we observed a wide range of phenotypic variation in both total lateral root length and total root length among the tested accessions (Fig. 1, A and B). The total lateral root length per plant ranged from 5 to 29.8 cm at high N (HN) and from 12.7 to 57.9 cm at LN (Fig. 1A; Supplemental Table S1). Similarly, the total root length per plant ranged from 9.7 to 39.9 cm at HN and from 16.2 to 69.5 cm at LN (Fig. 1B; Supplemental Table S1). Total lateral root length was closely correlated with total root length within N treatments, but to a weaker extent across N treatments (Supplemental Table S2). The estimated broad-sense heritability (H^2) was 0.885 and 0.894 for HN and LN, respectively. On average, total lateral root length and total root length of all examined accessions at LN compared to HN increased by 100% and 70%, respectively ($P < 2.2e{-}16$; Fig. 1, A and B).

To address whether LN-stimulated root growth allows plants to capture more N, we measured N contents in the shoots as a proxy for total N uptake. Shoot N contents in the 200 accessions ranged from 24.0 to 92.3 μg

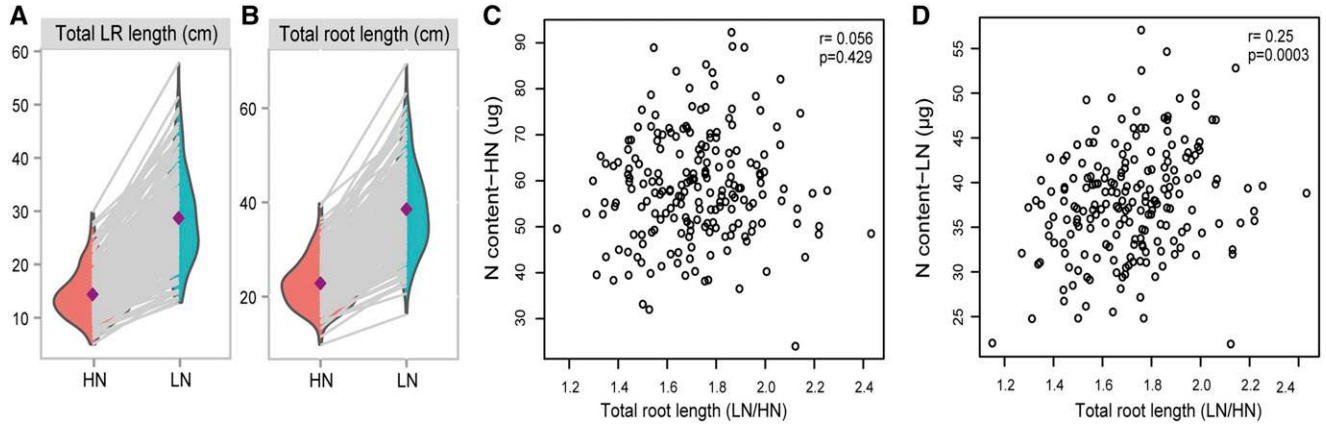

Figure 1. Natural variation of total lateral root length and total root length under two N environments. A and B, Reaction norms and phenotypic variation of total lateral root (LR) length (A) and total root length (B) of 200 natural accessions of Arabidopsis under different N supply. Purple diamonds represent means of total lateral root length and total root length under each N treatment. C and D, Correlations of total root length (i.e. LN-to-HN ratio) with shoot N content at HN (C) and LN (D). Seven-day-old seedlings precultured on 11.4 mM N were transferred to solid agar media containing either HN (11.4 mM N) or LN (0.55 mM N). Total lateral root length and total root length were determined after 9 d.

at HN and from 21.9 to 57.1 μg at LN (Supplemental Fig. S1). We then correlated the response of total root length (i.e. the ratio of total root length under LN and HN) with shoot N contents (Fig. 1, C and D). Whereas under HN conditions there was no significant correlation, a significantly positive correlation was found under LN, supporting the view that the altered root system architecture induced by mild N deficiency can increase N uptake and help plants to better adapt to this environmental constraint.

GWA Mapping Associates Natural Variation of Total Lateral Root Length and Total Root Length under LN with *DWF1*

In order to identify causative genetic loci for the variation of total lateral root length and total root length, we performed a GWA study. We did not detect any significant single nucleotide polymorphisms (SNPs) for either trait in either of the two N environments that exceeded the stringent significance threshold after Bonferroni correction of 5%. However, as complex traits are usually controlled by multiple genes, with small to moderate effects (Kooke et al., 2016), true associations may be missed for certain traits by using such a conservative threshold. In fact, by also considering slightly lower significance levels, at HN we mapped two groups of SNPs on chromosome 5 with $-\log_{10}$ (*P*-value) of 4.85 and 4.89 (Supplemental Fig. S2). These SNPs were located on *ANTHRANILATE SYNTHASE ALPHA SUBUNIT1/WEAK ETHYLENE INSENSITIVE2* (*ASA1/WEI2*; three SNPs at positions 1,720,343, 1,721,662, and 1,721,826 bp) or close to *miRNA166* (two SNPs at position 16,756,603 and 16,756,753 bp). Both *ASA1/WEI2* and *miRNA166* have been previously shown to regulate root development (Sun et al., 2009; Carlsbecker et al., 2010). In agreement with the study of Sun et al. (2009), we also observed that the *wei2-2* mutant exhibits a shorter primary root and forms fewer lateral roots than the wild type, which resulted in a significantly decreased total root length under HN and LN (Supplemental Fig. S3). These results suggested that further hidden true associations can be uncovered by using a lower significance threshold.

We then used a less stringent arbitrary threshold of significance for $-\log_{10}$ (*P*-value) of 5 for the data obtained at LN. We identified a total of six SNPs to associate with total lateral root length and total root length under LN, with five associations on chromosome 3 and one on chromosome 1 (Fig. 2). The most significant association, which explained 7.7% and 12.8% of the observed phenotypic variation for total lateral root length and total root length, respectively, was detected on chromosome 3 (at 6,869,961 bp). To identify the causal gene underlying this association, the linkage disequilibrium (LD) support interval ($r^2 > 0.6$), spanning from 6,867,572 to 6,890,191 bp and including seven genes, was determined (Supplemental Fig. S4). Among these genes, *DWF1* (At3g19820) raised major interest, because it encodes an enzyme catalyzing an early step in BR biosynthesis (Klahre et al., 1998; Youn et al., 2018). More importantly, its known function in cell elongation (Takahashi et al., 1995) is highly consistent with the stimulatory growth effect at LN, which increases root length through cell elongation (Jia et al., 2019). Nonetheless, in an unbiased approach, we phenotyped transfer DNA (T-DNA) knockout lines for all genes in the interval, except for AT3G19810, whose homozygous knockout is embryo lethal (Yang et al., 2016). The total root length of insertion lines for all genes except *DWF1* was comparable to the wild type irrespective of the N condition (Supplemental Fig. S4B). We observed that mutants of *DWF1* (*cabbage1* [*cbb1*] and *dwf1*) showed shorter primary and lateral roots under

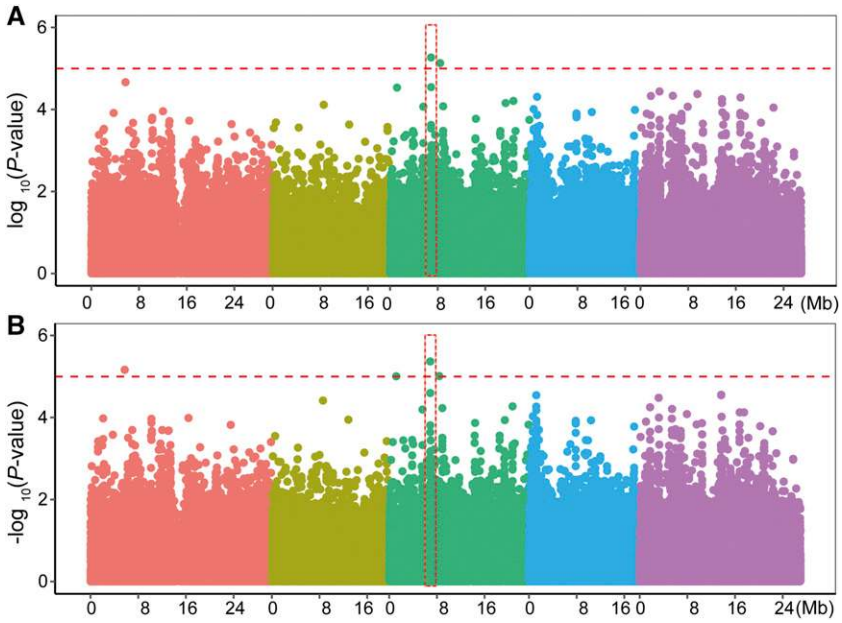

Figure 2. GWA maps the natural variation of total lateral root length and total root length under LN to *DWF1*. A and B, Manhattan plots were performed with the EMMA package to determine SNP associations with total lateral root length (A) and total root length (B) under LN. Negative $\log_{10}$-transformed *P*-values from a genome-wide scan were plotted against positions on each of the five chromosomes of Arabidopsis. Chromosomes I to V are depicted in different colors from left to right. The red dashed line corresponds to the arbitrary threshold of $-\log_{10}$ (*P*-value) = 5. The genomic region associated with the *DWF1* locus is framed in red.

either N condition; in particular, the N-deficiency response for average lateral root length, i.e. the relative increase from HN to LN, was attenuated by 28% and 24% for *cbb1* and *dwf1*, respectively (Fig. 3, A–E). As a consequence, the response of total root length to LN in these mutants decreased by 19% and 14% compared to their respective wild types (Fig. 3, F and G). To further investigate the possible role of *DWF1* in the regulation of root growth responses to LN, root system architectural traits were analyzed in *DWF1* RNA interference (RNAi) and overexpression lines (Fig. 4A). At HN, primary root, average lateral root, and total root lengths were significantly decreased by *DWF1* knockdown but significantly increased by *DWF1* overexpression compared to the wild type, Col-0 (Fig. 4, B–E; Supplemental Fig. S5, A–C). At LN, overall root elongation of *DWF1* knockdown lines was only slightly increased, while Col-0 and *DWF1* overexpressing lines exhibited similarly strong root elongation responses. However, in contrast to HN, an additional stimulatory effect of *DWF1* overexpression in the Col-0 background was not observed (Fig. 4, B–E; Supplemental Fig. S5, D–F). Taken together, these results indicate that *DWF1* is involved in the root elongation response induced by mild N deficiency and strongly suggest that *DWF1* is the causal gene underlying the marker-trait association on chromosome 3 (Chr 3_6869961; Fig. 2).

To investigate whether the inability of *dwf1* mutants to respond to LN was eventually due to general impairment of cell elongation, we assessed root responses of *dwf1* mutants to nitrate, a condition that stimulates cell elongation and root elongation (Liu et al., 2013). As expected, the elongation of primary and lateral roots in Col-0 and *dwf1* was stimulated by nitrate as compared to ammonium (Supplemental Fig. S6). In contrast, responses of lateral and total root length to LN were attenuated in *dwf1* plants (Supplemental Fig. S7), which exhibited comparable or even slightly higher stimulation of root elongation compared to the wild type when grown under nitrate (Supplemental Fig. S6). These results show that nitrate-induced cell and root elongation were not impaired in the *dwf1* mutant and thus rule out that a general BR-dependent defect in cell elongation was responsible for the compromised root response of *DWF1*-defective mutants to mild N deficiency. We then tested the importance of BR biosynthesis in the root foraging response to LN by different natural accessions. In the weakly responding lines Co and Kz-9, the exogenous supply of brassinazole (BRZ), an inhibitor of BR biosynthesis (Asami et al., 2000), had little impact on the response of total root length, average lateral root length, and primary root length to LN (Fig. 5). However, in six N-responsive accessions LN-induced root responses were strongly attenuated by BRZ (Fig. 5), suggesting that genetic variation in endogenous BR levels is associated with root architectural responses to LN.

Noncoding Variation at the *DWF1* Locus Is Causal for Natural Variation of Root Length at LN

Identification of *DWF1* by GWA suggested that allelic variation in *DWF1* associates with phenotypic variation of root length. However, the SNP linked with our GWA study was 10 kb away from the *DWF1* coding region, and SNPs in closer vicinity to the *DWF1* coding region did not show any significant association, pointing to the possibility that allelic heterogeneity and multiple variants in the *DWF1* locus contribute to natural variation of root growth. We next searched for SNPs among the *DWF1* genomic sequences available for 139 of the 200 natural accessions phenotyped in this study and performed a local *DWF1*-based association analysis. Considering a genomic region including a 2-kb-long promoter sequence, the full coding sequence,

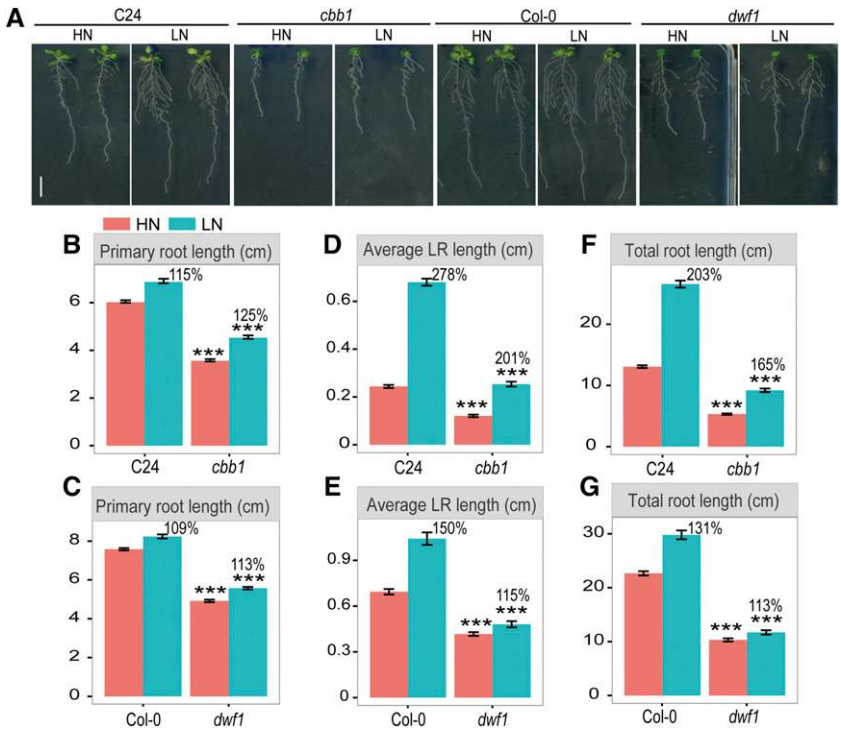

Figure 3. Root architecture of two *dwf1* mutants in response to LN. Plant appearance (A), primary root length (B and C), average lateral root (LR) length (D and E), and total root length (F and G) are shown in two mutant lines (*cbb1* and *dwf1)* and their corresponding wild types (C24 and Col-0). Seven-day-old seedlings were precultured on 11.4 mM N and then transferred to solid agar media containing either HN (11.4 mM N) or LN (0.55 mM N). Root system architecture was assessed after 9 d. Bars represent means ± SE (n = 16–24 plants). Numbers over columns indicate percent changes under LN versus HN for root length. Asterisks indicate statistically significant differences between mutants and wild types according to Welch's t test (***$P < 0.001$). Scale bar = 1 cm.

and a 0.4-kb-long 3′-untranslated region, we identified a total of 27 polymorphic sites (minor allele frequency >5%) including SNPs and insertions/deletions (Indels; Supplemental Table S3). Using a generalized linear model (GLM), we detected three SNPs (−1,808T/A, −1,304T/G and −984T/A) in the promoter region that were significantly associated with total lateral root length and total root length at HN, with −984T/A showing the most significant association (Fig. 6A; Supplemental Fig. S8A; Supplemental Table S4). At LN, one additional significant

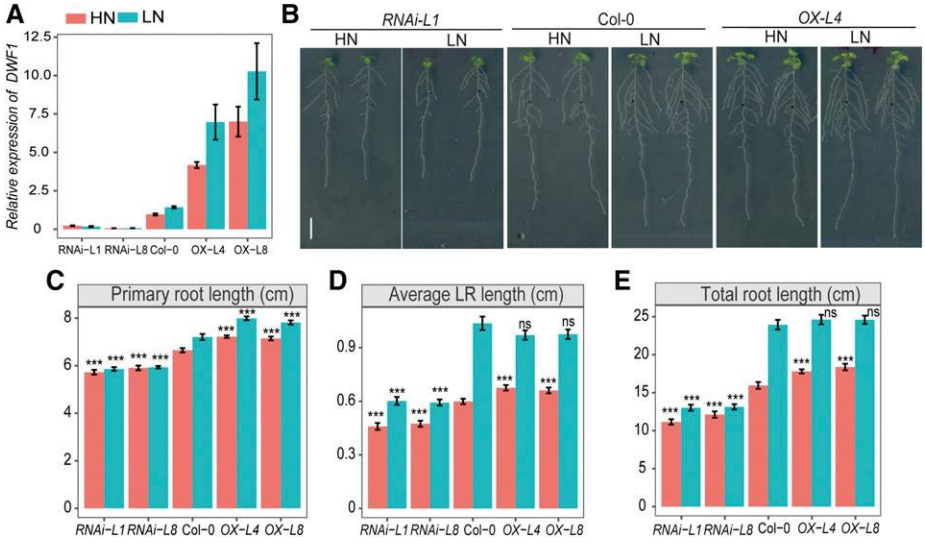

Figure 4. Root architecture of *DWF1* RNAi and overexpressing (OX) lines in response to LN. A, Transcript levels of *DWF1* in transgenic lines grown under HN (11.4 mM N) or LN (0.55 mM N). Gene expression levels were assessed in whole roots by RT-qPCR and normalized to *ACT2* and *UBQ10*. Bars represent means ± SE (n = 3 independent biological replicates). B to E, Appearance of plants (B), primary root length (C), average lateral root (LR) length (D), and total root length (E) of wild-type Col-0 and *DWF1* transgenic lines. Seven-day-old seedlings were precultured on 11.4 mM N and then transferred to solid agar media containing either HN or LN. *DWF1* expression levels and root system architecture were assessed after 9 d. Bars represent means ± SE (n = 18–24 plants). Asterisks indicate statistically significant differences between the wild type and transgenic lines according to Welch's t test (***$P < 0.001$; ns, not significant). Scale bar = 1 cm.

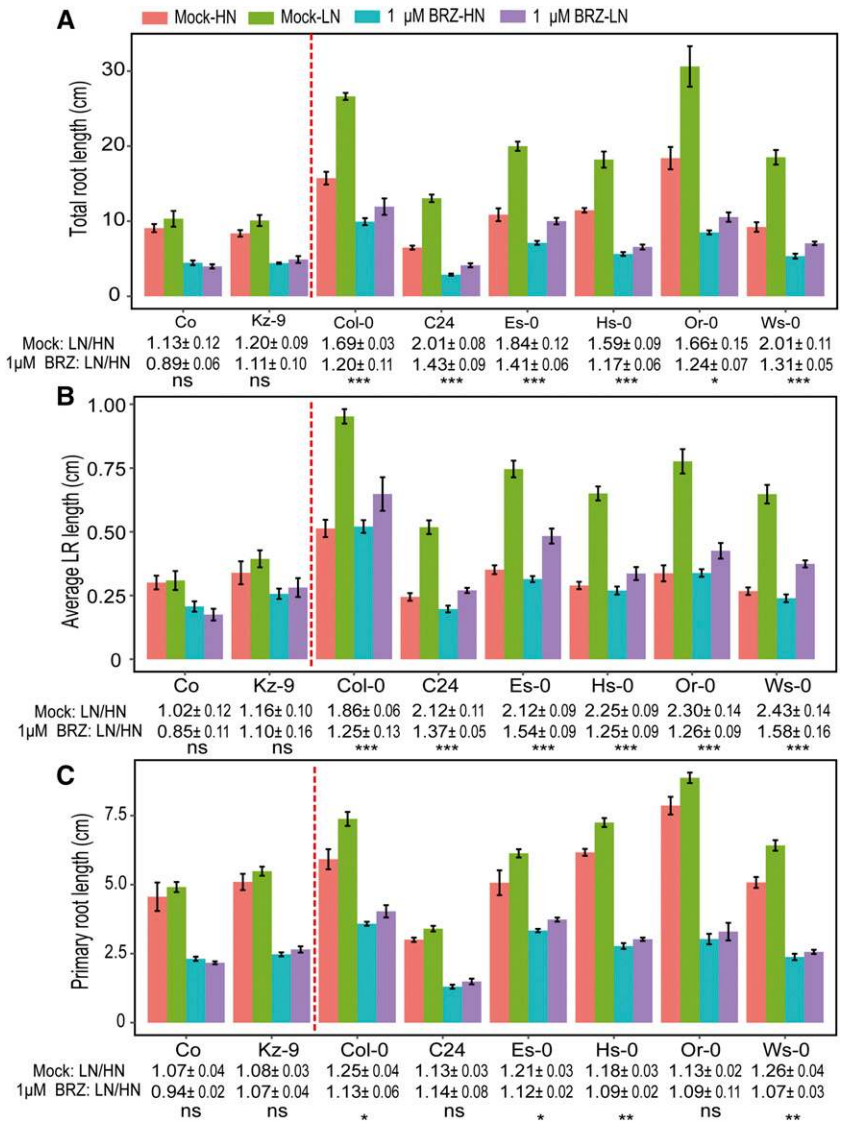

Figure 5. Differential sensitivity of root length to inhibition of BR biosynthesis in natural accessions. Total root length (A), average lateral root (LR) length (B), and primary root length (C) in accessions, showing contrasting root length responses to LN (two weak and six strong responders). Seven-day-old wild-type seedlings were precultured on 11.4 mM N and then transferred to solid agar media containing either HN (11.4 mM N) or LN (0.55 mM N) in the absence or presence of 1 μM BRZ. Root system architecture was assessed after 9 d. Bars represent means ± SE (n = 8–11 plants). Red dashed lines distinguish accessions into weakly (left) and strongly (right) responding lines. Asterisks indicate significant differences between relative root length (i.e. ratio of LN to HN) grown under BRZ and mock treatments according to Welch's t test (*$P < 0.05$, **$P < 0.01$, and ***$P < 0.001$; ns, not significant).

SNP (−1,329G/T) was detected, while −984T/A became even more significantly associated with root length. Identification of these multiple associations in the promoter of *DWF1* corroborated that allelic heterogeneity at the *DWF1* locus contributes to natural variation of root length.

In the next step, we used four SNPs detected in the *DWF1* locus to define five haplogroups (H1–H5), each encompassing 11 to 69 accessions (Fig. 6C; Supplemental Table S5). These haplogroups represented three phenotypic classes, in which H3 showed the most vigorous root growth at both HN and LN, while H2 showed intermediate growth and H1, H4, and H5 showed the least growth (Fig. 6D; Supplemental Fig. S8B). Importantly, accessions of H3, H2, and H1, H4, and H5 showed the strongest, intermediate, and weakest responses, respectively, of total lateral root length and total root length to LN (Fig. 6E; Supplemental Fig. S8C). These results suggest that genetic diversity in *DWF1* truly contributes to shaping differential root foraging responses in natural accessions. We then analyzed the transcript levels of *DWF1* in 13 representative accessions belonging to haplotypes 1, 3, 4, or 5. We found that, although indistinguishable at HN, relative transcript levels of *DWF1* were significantly higher in H3 accessions than in H1 and H5 at LN (Fig. 6F). Notably, we observed that *DWF1* expression at LN was significantly correlated to total lateral root length and total root length (Fig. 6G; Supplemental Fig. S8D). Altogether, these results indicate that noncoding variants of *DWF1* result in variable gene expression levels that, in turn, contribute to the natural variation of root growth at LN.

LN Upregulates *DWF1* Expression in Roots

To investigate how *DWF1* regulates root responses to LN, we performed reverse transcription quantitative PCR (RT-qPCR) analysis and found that expression of *DWF1* in Col-0 was significantly upregulated by LN (Fig. 7A). This response was additionally validated using a *proDWF1*::GUS reporter line, which revealed that *DWF1* promoter activity was increased in the apices of primary

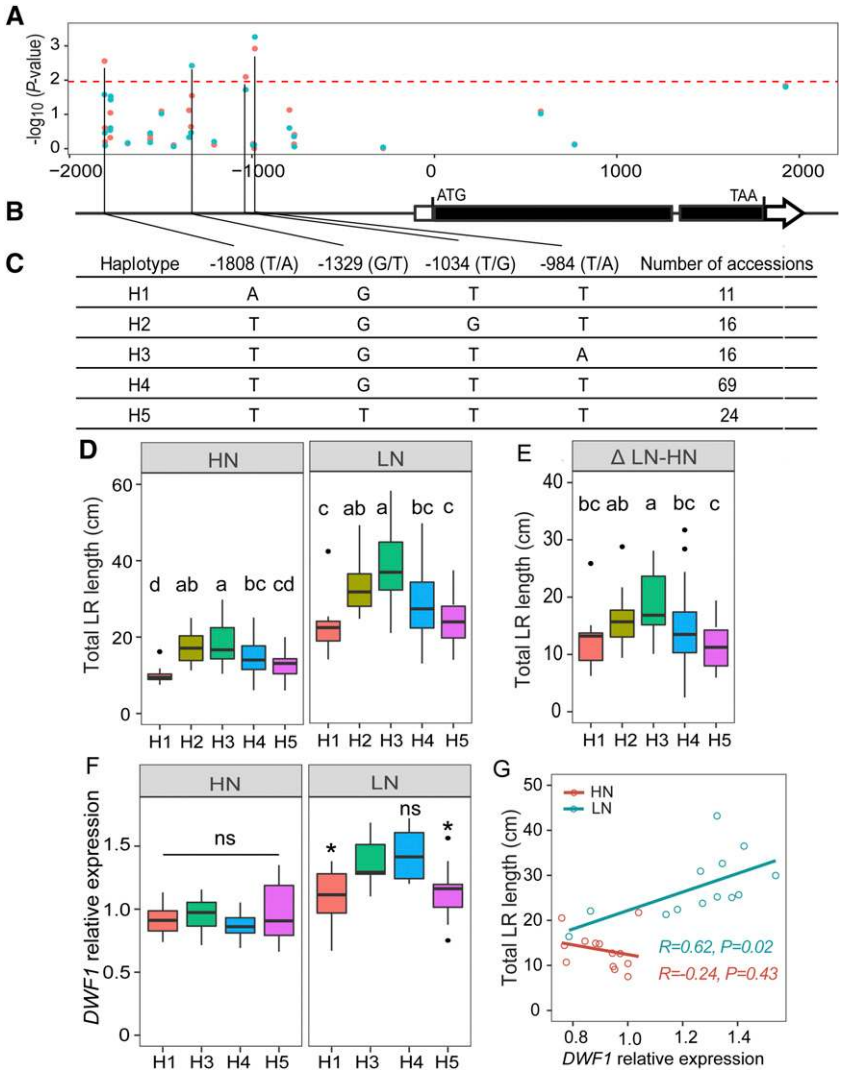

Figure 6. *DWF1*-based association analysis reveals allelic variation at the *DWF1* locus. A, Association between total lateral root length under HN (red) and that under LN (light blue) for 27 polymorphic sites (MAF >0.05) in the genomic region of *DWF1* in 139 resequenced accessions. The *x* axis shows the nucleotide position of each variant relative to the translation starting site ATG. The *y* axis shows the $-\log_{10}$ (*P*-value) for the association test using a generalized linear model. The dashed line indicates the significance level at $\alpha = 0.01$. B, Four polymorphisms selected for further analysis are projected onto a schematic representation of the *DWF1* gene structure. The boxes represent exons, with solid and empty boxes showing translated and untranslated regions, respectively. C, Representation of the four selected SNPs used to define five haplotypes (H1–H5) and number of accessions contained in each haplogroup. D, Total lateral root (LR) length for each haplogroup under HN and LN. E, Plasticity of total lateral root length for each haplogroup, as defined by the difference between LN and HN (ΔLN − HN). Lowercase letters indicate significant differences at $P < 0.05$ according to one-way ANOVA and post hoc Tukey's HSD mean-separation test. F, Gene expression of *DWF1* in accessions representing H1 (Ra-0, LL-0, and Bla-1), H3 (Got-7, Ha-0, Wa-1, and Blh-1), H4 (Co, Sha, and Kin-0), and H5 (Edi-0, Rmx-A180, and Se-0) at HN or LN. *DWF1* expression levels were assessed in whole roots by RT-qPCR analysis and normalized to *ACT2* and *UBQ10*. Shown are data from three independent biological replicates for each accession. Asterisks indicate statistically significant differences between H3 and others according to Welch's *t* test (*$P < 0.05$; ns, not significant). G, Correlation of *DWF1* transcript levels in roots with total LR length at both N conditions.

roots, and especially in mature lateral roots, when plants were grown under LN (Fig. 7B). To better understand the role of *DWF1* in LN-induced lateral root development, *DWF1* promoter activity was also monitored in lateral roots at different developmental stages. There was no detectable GUS staining in non-emerged or just emerged lateral root primordia (Fig. 7, C and D). However, *DWF1* promoter activity increased as soon as lateral roots started to elongate (Fig. 7E). More intense GUS staining was observed in the elongation and maturation zone of lateral roots grown under LN compared to HN (Fig. 7, F and G). Altogether, these data suggest that *DWF1* expression is induced by LN and confined to the root elongation zone.

Enhanced Root Elongation under LN Depends on BR Biosynthesis and Its Upregulation by LN

Previous studies identified *DWF1* as encoding a C-24 reductase that catalyzes the conversion of 24-methylenecholesterol to campesterol and (6-deoxo) dolichosterone to (6-deoxo)castasterone in the BR biosynthesis pathway (Klahre et al., 1998; Youn et al., 2018). To investigate whether the attenuated root response in *cbb1* and *dwf1* mutants is caused by perturbed BR biosynthesis, the bioactive BR 24-epibrassinolide (BL) was exogenously supplied to plants. Irrespective of the external N availability, the absolute primary root length of the wild-type C24 continuously decreased with increasing BL concentrations (Fig. 8, A and B). In contrast, the *cbb1* mutant was less sensitive to repression by BL and increased primary root length, confirming that *cbb1* plants were not able to maintain near-optimal endogenous BR levels for root growth without external BL supply (Fig. 8, A and B). In contrast to the primary root, 1 nM BL stimulated the average lateral root length of wild-type and *cbb1* plants under both N regimes (Fig. 8, A and C). Notably, total root length and average lateral root length of C24 at LN were significantly repressed at BL concentrations >1 nM, whereas they were hardly affected in *cbb1* and HN-grown C24 plants (Fig. 8, C and D), which is consistent with the

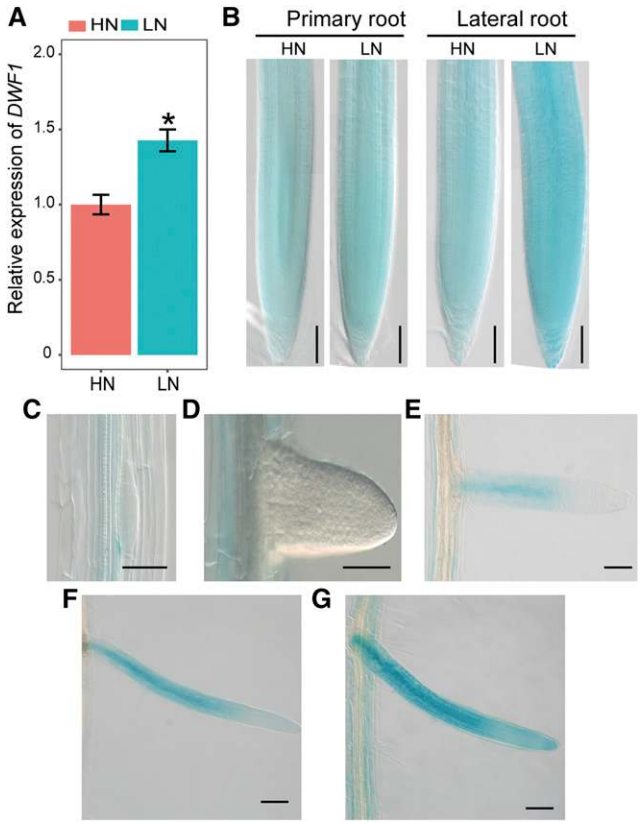

Figure 7. Expression of *DWF1* in roots under LN. A, *DWF1* transcript levels in response to HN or LN availabilities. *DWF1* expression levels were assessed in whole roots of Col-0 by RT-qPCR analysis and normalized to *ACT2* and *UBQ10*. Bars represent means ± SE ($n = 3$ independent biological replicates) and asterisks indicate statistically significant differences between two N environments according to Welch's *t* test (*$P < 0.05$). B, *proDWF1*-dependent GUS activity in the Col-0 background assessed in primary and lateral root tips. C to E, *proDWF1*-dependent GUS activity during different stages of lateral root development under HN. F and G, *proDWF1*-dependent GUS activity in elongating lateral roots grown under HN (F) or LN (G). Seven-day-old seedlings were precultured on 11.4 mM N and then transferred to solid agar containing either HN (11.4 mM N) or LN (0.55 mM N). Samples for RT-qPCR analysis and GUS activity assays were taken 9 d after transfer. Scale bars = 100 μm.

previous finding that BR sensitivity is enhanced at LN (Jia et al., 2019). Most importantly, the response of average lateral root length and total root length at LN were completely rescued by application of 10 or 50 nM BL (Fig. 8, C and D). These results indicate that mild N deficiency enhances BR biosynthesis to promote root elongation.

To further verify whether LN promotes BR biosynthesis, we assessed the expression of *CONSTITUTIVE PHOTOMORPHOGENIC DWARF* (*CPD*), *DWF4*, and *BRASSINOSTEROID-6-OXIDASE2* (*BR6OX2*), three genes encoding central enzymes in the BR biosynthetic pathway. According to RT-qPCR analysis of whole roots, expression levels of all three genes were significantly upregulated in roots by mild N deficiency (Fig. 9A). Moreover, we found that the responses of primary and lateral roots to LN was significantly attenuated in *cpd* and *dwf4* mutants (Fig. 9, B–D; Supplemental Fig. S9). Consequently, these mutants also failed to significantly increase total root length at LN (Fig. 9E; Supplemental Fig. S9D). Given that the *cpd* and *dwf4* mutants show impaired growth under many conditions, we examined whether root elongation under LN is simply associated with general BR-dependent growth defects. We gradually repressed BR biosynthesis of Col-0 plants by supplying increasing concentrations of BRZ. As expected, shoot and root growth decreased with increasing BRZ levels at either N condition (Supplemental Fig. S10A). However, very low BRZ supply (0.1 μM) strongly inhibited root growth and repressed lateral root and total root length under LN, while its impact on shoot growth remained marginal (Supplemental Fig. S10, B–E). Thus, LN-induced BR biosynthesis is crucial to stimulate root elongation in response to mild N deficiency, which argues against the assumption that the lack of response of BR biosynthesis mutants to LN was due to a general effect of BRs on growth. Altogether, these results further indicated that LN stimulates root growth via upregulation of particular BR biosynthesis genes.

Our initial correlation analyses indicated that larger root size improves overall N uptake, especially at LN (Fig. 1, C and D). To further verify whether altered root size affects N uptake, *DWF1* transgenic lines were analyzed for shoot growth and N content. At HN, knockdown lines of *DWF1* exhibited a significant reduction in shoot biomass of 17% to 22%, whereas at LN, shoot biomass accumulation in *DWF1* RNAi lines decreased by 32% to 35% relative to the wild type (Fig. 10A), suggesting an important role of *DWF1* in plant growth adaptation to LN. Compared to Col-0, overexpression of *DWF1* increased shoot growth by 18% to 22% and 15% to 20% at HN and LN, respectively. Altered expression of *DWF1* had no impact on shoot N concentrations at either N-supply level (Fig. 10B). Accordingly, shoot N content followed shoot biomass and was lower in the RNAi lines and higher in the overexpression lines (Fig. 10C). Taken together, we conclude that *DWF1* plays a key role in adaption to LN and that enhanced expression of *DWF1* can improve aboveground N accumulation mainly via enhanced biomass.

DISCUSSION

Previous studies have shown that in combination with local signals, systemic signals also modulate phytohormone biosynthesis, transport, or signaling to coordinate root system architectural changes under varied N availability (Vidal et al., 2010; Giehl and von Wirén, 2014; Ristova et al., 2016). The root foraging response observed under mild N deficiency relies on the elongation of both primary and lateral roots and is driven in part by enhanced BR signaling (Jia et al.,

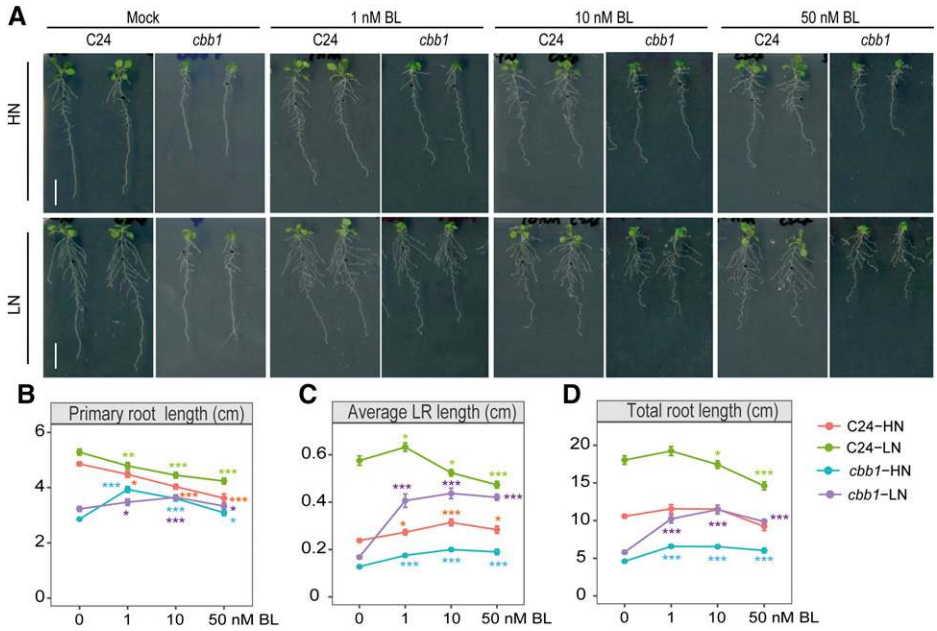

Figure 8. Exogenous BR supply rescues root elongation of *cbb1* mutant at LN. Plant appearance (A), primary root length (B), average lateral root length (C), and total root length (D) are shown for wild-type (C24) and *cbb1* mutant plants. Seven-day-old seedlings were precultured on 11.4 mM N and then transferred to solid agar media containing either HN (11.4 mM N) or LN (0.55 mM N) supplemented or not with BL at the indicated concentrations. Root system architecture was assessed after 9 d. Bars represent means ± SE (n = 15–20 plants). Asterisks indicate significant differences between exogenous BR supply and mock treatment according to Welch's t test (*$P < 0.05$, **$P < 0.01$, and ***$P < 0.001$). Scale bars = 1 cm.

2019). So far, the role of BR biosynthesis in this adaptive response has remained elusive. Here, we show that mild N deficiency induces central genes in BR biosynthesis and that natural variation in the BR synthesis gene *DWF1* contributes to the extent of this root foraging response under LN.

BRs are a class of naturally occurring polyhydroxylated steroidal hormones that are of crucial importance for physiological and developmental adaptations of plants to environmental conditions (Wang et al., 2012b). Recently, substantial evidence has been provided that BRs are involved in low iron- or temperature-dependent root growth processes (Singh et al., 2014, 2018; Martins et al., 2017). BRs are mostly considered to be growth-promoting phytohormones, as shown e.g. by hypocotyl elongation of light-grown

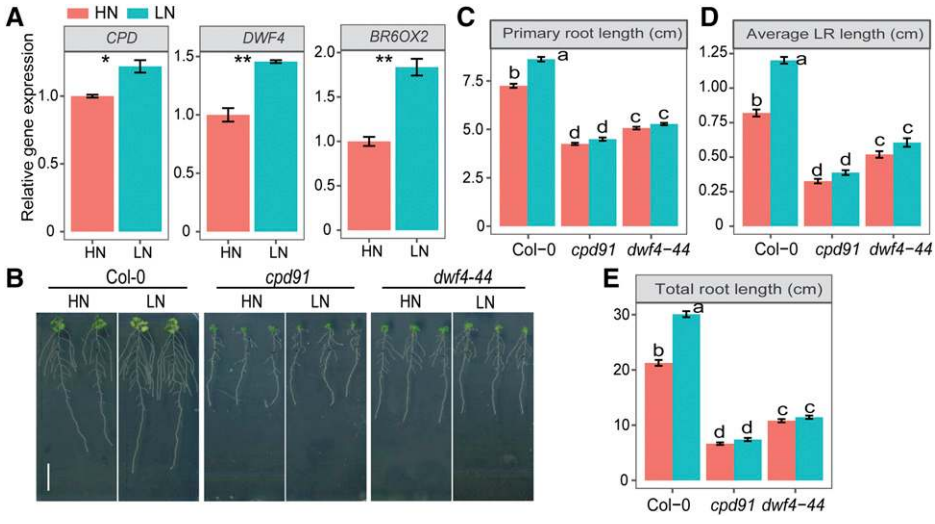

Figure 9. Expression of genes involved in BR biosynthesis and N-dependent root architecture of the corresponding mutants. A, Transcript levels of *CPD*, *DWF4*,, and *BR6OX2* in response to N availability. Gene expression levels were assessed in whole roots by RT-qPCR analysis and normalized to *ACT2* and *UBQ10*. Bars represent means ± SE (n = 3 independent biological replicates) and asterisks indicate statistically significant differences between two N environments according to Welch's t-test (*$P < 0.05$ and **$P < 0.01$). B to E, Appearance of plants (B), primary root length (C), average lateral root (LR) length (D), and total root length (E) of wild-type (Col-0), *cpd91*, and *dwf4-44* mutant plants. Seven-day-old seedlings were precultured on 11.4 mM N and then transferred to solid agar media containing either HN (11.4 mM N) or LN (0.55 mM N). Root system architecture was assessed after 9 d. Bars represent means ± SE (n = 12–25 plants). Lowercase letters indicate significant differences at $P < 0.05$ according to one-way ANOVA and Tukey's HSD mean-separation test. Scale bar = 1 cm.

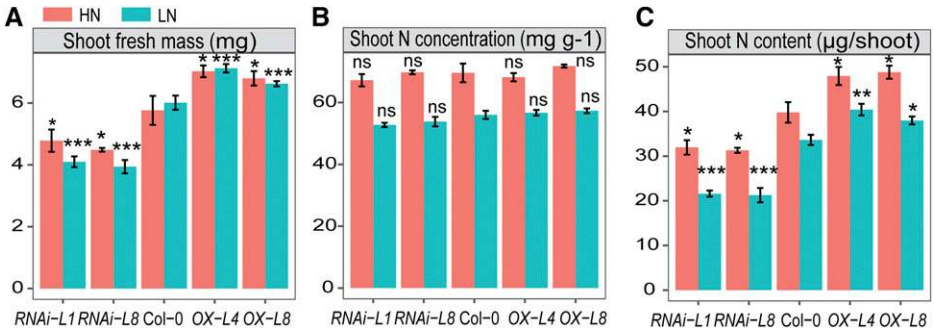

Figure 10. Overexpression of *DWF1* improves shoot growth and N accumulation. Shoot fresh mass (A), N concentration (B), and N content (C) of the wild type (Col-0), two *DWF1* RNAi lines, and two *DWF1* overexpressing (OX) lines. Seven-day-old seedlings were precultured on 11.4 mM N and then transferred to solid agar media containing either HN (11.4 mM N) or LN (0.55 mM N). Shoot fresh mass and N concentrations were assessed after 9 d. Bars represent means ± SE ($n = 4$ replicates). Asterisks indicate statistically significant differences between the wild-type and transgenic lines according to Welch's *t* test (*$P < 0.05$, **$P < 0.01$ and ***$P < 0.001$; ns, not significant).

seedlings subjected to exogenous application of BL or by genotypes with enhanced BR signaling that produce longer hypocotyls (Wang et al., 2012b). However, this positive response does not hold true for root growth in all cases. While it has been shown that low iron stimulates root elongation by activating BR signaling (Singh et al., 2018), elevated ambient temperature downregulates BR signaling to promote root elongation (Martins et al., 2017), suggesting a complex scenario for the role of BRs in the regulation of root growth responses to different environmental cues. Nonetheless, both studies suggested that root elongation in response to low iron and elevated ambient temperature is not dependent on hormone ligands, since mutants impaired in BR biosynthesis, like *deetiolated2* (*det2*), *cpd*, and *dwf4* were still responsive to iron deficiency or ambient high temperature (Martins et al., 2017; Singh et al., 2018). In contrast, BR biosynthesis and signaling are concomitantly downregulated under long-term phosphate deficiency to inhibit root elongation (Singh et al., 2014).

Against the background that BR signaling contributes to root elongation under mild N deficiency (Jia et al., 2019), we provide evidence here that in addition, BR synthesis is crucial for the root foraging response under LN. Through GWA mapping, we found that at LN, *DWF1* is associated specifically with total lateral root length and total root length (Fig. 2; Supplemental Fig. S2). *DWF1* encodes a Ca^{2+}-dependent calmodulin-binding protein that was initially demonstrated to be a sterol C-24 reductase that converts 24-methylelecholesterol to campesterol, which is the first precursor in C-28 BR formation (Klahre et al., 1998; Du and Poovaiah, 2005). More recently, it has been shown in Arabidopsis that DWF1 possesses additional enzyme activity as BR C-24 reductase, catalyzing C-24 reduction of 6-deoxodolichosterone and dolichosterone to 6-deoxocastasterone and castasterone, respectively (Youn et al., 2018). Accordingly, *dwf1* null mutant plants showed a significant reduction in the bioactive BR species castasterone (Youn et al., 2018). Our phenotypic characterization of *dwf1* null alleles and RNAi lines indicated that functional DWF1 is required for root elongation in response to mild N deficiency (Figs. 3 and 4; Supplemental Figs. S5 and S7). In agreement with the observation that exogenous application of biologically active BL successfully reverted the root response of the *cbb1* mutant to LN (Fig. 8), we conclude that BR deficiency in *DWF1*-defective mutant plants causes the impaired root response to LN. Importantly, lowering endogenous BR levels either by mutation of central BR biosynthesis genes, such as *CPD* and *DWF4*, or by exogenous supply of the BR biosynthesis inhibitor BRZ significantly attenuated low N-induced root elongation (Figs. 5 and 9; Supplemental Figs. S9 and S10). In addition, transcript levels of *DWF1*, *CPD*, *DWF4*, and *BR6OX2* were significantly upregulated at LN (Figs. 7 and 9A), indicating that several steps in BR biosynthesis are enhanced. Taken together, these results indicate that expression of key genes in the biosynthetic pathway of BRs is upregulated in response to LN to increase BR levels as a prerequisite for subsequent root elongation. Interestingly, it has been observed recently that in rapeseed (*Brassica napus*) roots, which also elongate under N deficiency, DWF1 protein abundance was significantly enriched under N-deficient conditions (Qin et al., 2019), suggesting that BRs play a conserved role across plant species in the root foraging response at LN.

Phenotypic variation in root traits among accessions may rely on allelic variation driving gene transcription or changing protein function. For instance, variation at the locus of *FERRIC REDUCTION OXIDASE2* (*FRO2*) alters its transcript level that is associated with iron-dependent root growth (Satbhai et al., 2017), while the occurrence of one nonsynonymous substitution in BSK3 differentiates BR signaling in the control of phenotypic variation of root elongation under mild N deficiency (Jia et al., 2019). Here, we detected a number of SNPs in the promoter region of *DWF1* that significantly

associate with total lateral root length and total root length, allowing us to categorize 139 of the assessed accessions in five different haplogroups (Fig. 6, A–C; Supplemental Fig. S8A). Interestingly, accessions belonging to these haplogroups to a large degree exhibited distinct root length and root responsiveness to LN (Fig. 6, D and E; Supplemental Fig. S8, B and C), suggesting that noncoding variation at the *DWF1* locus is causal for the observed natural variation of root length. This conclusion is further supported by the positive and significant correlation between *DWF1* transcript levels in different *DWF1* haplotypes and root length under LN conditions (Fig. 6G; Supplemental Fig. S8D). Thus, variation in *DWF1* expression likely causes variation in endogenous BR levels and in the corresponding phenotypic root response. Supporting this notion, root foraging responses of accessions with strong responses to LN were significantly compromised when endogenous BR biosynthesis was blocked by exogenous BRZ supply (Fig. 5). Noteworthy, *DWF1* locus-associated allelic variation contributed ~7.7% to the overall variation of total lateral root length under LN (Fig. 2), while *BSK3*-dependent allelic variation contributed ~12% to natural variation in primary root length under LN (Jia et al., 2019). Thus, further regulatory pathways must be involved in determining the extent of the root foraging response to LN.

Developing longer primary and lateral roots to increase root size is commonly observed in many plant species that are suffering from N limitation or depletion in soils (Chun et al., 2005; Gruber et al., 2013; Ma et al., 2014; Shao et al., 2017; Qin et al., 2019). Whether such an enlarged root system is indeed beneficial for N acquisition by roots is not well documented and is difficult to prove in soil-grown plants. By assessing root architectural traits and shoot N accumulation as proxy for total N uptake, we found that changes in the root system size under LN are significantly and positively correlated with above-ground N accumulation in Arabidopsis (Fig. 1; Supplemental Fig. S1), suggesting that an extensive root system confers an advantage for N uptake especially at LN. In fact, this was also genetically verified by an association of root size with above-ground N accumulation when expression levels of *DWF1* were altered (Fig. 10). Knockdown of *DWF1* expression significantly decreased overall N accumulation, whereas overexpression enhanced it, under both high and LN conditions due to altered biomass formation. Recently, overexpression of the auxin biosynthesis gene *TaTAR2.1* in wheat (*Triticum aestivum*) greatly improved root growth as well as aboveground N accumulation and grain yield (Shao et al., 2017). That overexpressing *DWF1* significantly increased root growth at HN while maintaining it at LN (Fig. 4; Supplemental Fig. S5) suggests that *DWF1* could be a promising target for molecular breeding approaches. For the sake of enhanced N fertilizer use efficiency in agricultural plant production, uncoupling suppression of *DWF1* by high N doses, e.g. via ectopic expression, may allow growth of crops with more extensive root systems even in highly fertile soils, when sufficient amounts of N are available.

MATERIALS AND METHODS

Plant Materials and Growth Conditions

The Arabidopsis (*Arabidopsis thaliana*) accessions Col-0 and C24 were used as wild types in this study. The T-DNA knockout lines *dwf1* (SALK_006932), *cpd91* (SALK_078291), *cpd* (SALK_023532), *dwf4-44* (SAIL_882_F07), *dwf4* (SAIL_98_C12), SALK_127381C, SALK_133165C, SALK_078826C, SALK_074983C, SALK_032827C, and *wei2-2* were purchased from the Nottingham Arabidopsis Stock Center. The *cbb1* mutant, DIM1/DWF1 promoter-GUS, RNAi and overexpression lines in the background of Col-0 have been described in previous studies (Schluter et al., 2002; Hossain et al., 2012). For surface sterilization, seeds were incubated in 70% (v/v) ethanol and 0.05% (v/v) Triton X-100 for 15 min and then dried in a clean bench. Seeds were sown on modified half-strength Murashige and Skoog medium, as described by Gruber et al. (2013), supplemented with 11.4 mM N (1 mM NH_4NO_3 and 9.4 mM KNO_3), 0.5% (w/v) Suc, 1% (w/v) Difco agar (Becton Dickinson), and 2.5 mM MES (pH 5.6) and then kept in darkness at 4°C for 2 d to synchronize germination. After stratification, agar plates containing seeds were placed vertically in a growth cabinet (Percival Scientific) under a 22°C/19°C, 10 h/14 h light/dark regime with light intensity adjusted to 120 μmol photons m^{-2} s^{-1}. In all experiments, 7-d-old seedlings of similar sizes were transferred to new plates with the same Suc, agar, and nutrient composition as described above but supplied with either HN (11.4 mM) or LN (0.55 mM). For the LN treatment, concentrations of NH_4NO_3 and KNO_3 were decreased to 4.3% (v/v) and 4.4% (v/v) of those contained in the HN condition, respectively. For assessment of root growth responses to nitrate, 7-d-old seedlings precultured under HN (11.4 mM) were transferred to new plates with the same nutrient composition as described above but with 2 mM of either NH_4Cl or KNO_3 as the sole forms of N supply. The osmotic potential of these media was maintained by adding KCl. Treatments with BL or BRZ were performed by transferring 7-d-old seedlings to one-half strength Murashige and Skoog medium supplemented with the indicated concentrations of BL (CAS no. 78821-43-9, Sigma) or BRZ (CAS no. 280129-83-1, Sigma) dissolved in pure ethanol or dimethyl sulfoxide, respectively. Identical concentrations of solvent were used as mock treatments.

GWA Mapping and Sequence Mining

For root length screening, we grew 200 accessions (Supplemental Table S1) on HN and LN agar plates (four individual plants per plate) and repeated the screening three times so that finally a total of 12 plants per accession were analyzed in either N condition. Overlapping roots were disentangled directly on agar plates and scanned using an Epson Expression 10000XL scanner (Seiko Epson) with a resolution of 300 dots per inch. Root length was measured using the WinRhizo Pro version 2009c (Regent Instruments). Average values calculated from 12 plants per line for 200 accessions were used as the phenotypic response for association mapping. GWA mappings were performed using a mixed linear model algorithm implemented in the Efficient Mixed-model Association (EMMA) package (Kang et al., 2008) and 250K SNP markers (Atwell et al., 2010; Horton et al., 2012) after filtering the data for SNPs with minor allele frequency ≥10%. For *DWF1*-based local association analysis, we downloaded from the 1001 Genome Project database (http://signal.salk.edu/atg1001/3.0/gebrowser.php) the genomic sequences of *DWF1* (a region encompassing the 2-kb promoter, the full coding region, and the 0.4-kb 3′-untranslated region) for 139 genome-resequenced accessions that were phenotyped in this experiment. Sequences of 139 accessions were aligned with ClustalW2.1 (http://bar.utoronto.ca) before we extracted polymorphic sites including SNPs and Indels at minor allele frequency >5%. Association analyses of polymorphic sites and root lengths were performed with TASSEL version 2.1 using a generalized linear model (Bradbury et al., 2007). The significance threshold was set to $P \leq 0.01$. Haplotypes were classified based on significantly associated SNPs according to *DWF1*-based association analysis, and only haplogroups with at least seven accessions were taken for further comparative analysis.

Shoot N Analysis

Plant shoots were sampled 9 d after transfer to HN or LN, then freeze dried and ground using a ball mill. Approximately 1 mg of material was taken for analysis, and N concentration was determined using an elemental analyzer (Euro-EA, HEKAtech).

Histological Analysis and Microscopy

Tissue-specific localization of *DIM1/DWF1* expression was investigated by histological staining of GUS activity in transgenic plants expressing *proDIM1-*

GUS, as described in Hossain et al. (2012). Root samples were incubated in 20 mg mL^{-1} (w/v) 5-bromo-4 chloro-3-indolyl-β-D-GlcA (X-gluc), 100 mM $NaPO_4$, 0.5 mM $K_3Fe(CN)_6$, 0.5 mM $K_4Fe(CN)_6$, and 0.1% (v/v) Triton X-100 at 37°C in the dark. Samples were mounted in clearing solution (chloral hydrate:water:glycerol 8:3:1) for 3 min and then imaged using differential interference contrast optics on a light microscope (Axio Imager 2, Zeiss).

RT-qPCR

Root tissues were collected by excision and immediately frozen in liquid N. Total RNA was extracted with RNeasy Plant Mini Kit (Macherey-Nagel). RT-qPCR reactions were conducted with the CFX348 Real-Time System and the Go Taq qPCR Master Mix SybrGreen I (Promega) using the primers listed in Supplemental Table S6. Relative expression was calculated according to Pfaffl (2001), and all genes were normalized to *AtACT2* and *AtUBQ10* as the internal reference.

Statistical Analysis

Root traits of different genotypes were analyzed by one-way ANOVA followed by Tukey's honestly significant difference (HSD) mean-separation test at $P < 0.05$. Pairwise comparisons were carried out using Welch's *t* test. All statistical analyses were performed in R (R Core Team, 2013).

Accession Numbers

Sequence data from this article can be found in the GenBank/EMBL data libraries under accession numbers AT3G19820 (*DWF1/CBB1/DIM1*); AT5G05690 (*CPD*); AT3G50660 (*DWF4*); AT3G30180 (*BR6OX2*); AT5G05730 (*ASA1/WEI2*); AT5G41905 (*MiRNA166*); AT3G19770; AT3G19780; AT3G19790; AT3G19800; and AT3G19830.

Supplemental Data

The following supplemental materials are available.

Supplemental Figure S1. Distribution of shoot N content in 200 accessions at HN and LN conditions.

Supplemental Figure S2. GWA scan for total lateral root length and total root length under HN.

Supplemental Figure S3. *wei2-2* plants exhibit root growth defects that are independent of N supply but have intact response to LN.

Supplemental Figure S4. Candidate genes in the genomic region surrounding *DWF1* and root phenotype of their T-DNA insertion lines.

Supplemental Figure S5. Time-dependent changes of root architectural traits in *DWF1* knockdown and *DWF1* overexpressing lines grown under different N availability.

Supplemental Figure S6. Root growth responses of the *dwf1* mutant to ammonium and nitrate.

Supplemental Figure S7. Time-dependent root growth responses of the *dwf1* mutant to LN.

Supplemental Figure S8. *DWF1*-based association with total root length.

Supplemental Figure S9. Root system architecture of *cpd* and *dwf4* mutant plants in response to LN.

Supplemental Figure S10. Shoot and root growth responses to low N of Col-0 plants grown in the presence of a BR biosynthesis inhibitor.

Supplemental Table S1. Geo-referenced Arabidopsis ecotypes with their total lateral root length and total root length under HN versus lLN.

Supplemental Table S2. Correlations of total root length and total lateral root length within and across N environments.

Supplemental Table S3. Summary table of SNPs and Indels identified in the *DWF1* locus at a minor allele frequency of >5%.

Supplemental Table S4. Summary of SNP-trait associations using a generalized linear model.

Supplemental Table S5. Haplotype analysis of natural *DWF1* variants.

Supplemental Table S6. Primers used in this study.

ACKNOWLEDGMENTS

We thank Jacqueline Fuge, Annett Bieber, Elis Fraust and Lisa Gruber, (Leibniz Institute of Plant Genetics and Crop Plant Research) for excellent technical assistance. We also thank Florian Schröder (Max Planck Institute of Molecular Plant Physiology) for sharing seeds of *cbb1* and Abdelali Hannoufa (Agriculture and Agri-Food Canada) for *DWF1promoter-GUS* seeds and *DWF1* knockdown and overexpression lines. We further thank Thomas Altmann and Rhonda C. Meyer (Leibniz Institute of Plant Genetics and Crop Plant Research) for providing seeds and SNP data for Arabidopsis accessions.

Received April 9, 2020; accepted April 30, 2020; published May 12, 2020.

LITERATURE CITED

Abel S (2017) Phosphate scouting by root tips. Curr Opin Plant Biol **39:** 168–177

Araya T, Miyamoto M, Wibowo J, Suzuki A, Kojima S, Tsuchiya YN, Sawa S, Fukuda H, von Wirén N, Takahashi H (2014) CLE-CLAVATA1 peptide-receptor signaling module regulates the expansion of plant root systems in a nitrogen-dependent manner. Proc Natl Acad Sci USA **111:** 2029–2034

Asami T, Min YK, Nagata N, Yamagishi K, Takatsuto S, Fujioka S, Murofushi N, Yamaguchi I, Yoshida S (2000) Characterization of brassinazole, a triazole-type brassinosteroid biosynthesis inhibitor. Plant Physiol **123:** 93–100

Atwell S, Huang YS, Vilhjálmsson BJ, Willems G, Horton M, Li Y, Meng D, Platt A, Tarone AM, Hu TT, et al (2010) Genome-wide association study of 107 phenotypes in *Arabidopsis thaliana* inbred lines. Nature **465:** 627–631

Badri DV, Vivanco JM (2009) Regulation and function of root exudates. Plant Cell Environ **32:** 666–681

Bouguyon E, Brun F, Meynard D, Kubeš M, Pervent M, Leran S, Lacombe B, Krouk G, Guiderdoni E, Zažímalová E, et al (2015) Multiple mechanisms of nitrate sensing by *Arabidopsis* nitrate transceptor NRT1.1. Nat Plants **1:** 15015

Bradbury PJZ, Zhang Z, Kroon DE, Casstevens TM, Ramdoss Y, Buckler ES (2007) TASSEL: Software for association mapping of complex traits in diverse samples. Bioinformatics **23:** 2633–2635

Carlsbecker A, Lee JY, Roberts CJ, Dettmer J, Lehesranta S, Zhou J, Lindgren O, Moreno-Risueno MA, Vatén A, Thitamadee S, et al (2010) Cell signalling by microRNA165/6 directs gene dose-dependent root cell fate. Nature **465:** 316–321

Chun L, Mi GH, Li JS, Chen FJ, Zhang FS (2005) Genetic analysis of maize root characteristics in response to low nitrogen stress. Plant Soil **276:** 369–382

Drew MC (1975) Comparison of effects of a localized supply of phosphate, nitrate, ammonium and potassium on growth of seminal root system, and shoot, in barley. New Phytol 479–490

Du L, Poovaiah BW (2005) Ca^{2+}/calmodulin is critical for brassinosteroid biosynthesis and plant growth. Nature **437:** 741–745

Forde BG (2014) Nitrogen signalling pathways shaping root system architecture: An update. Curr Opin Plant Biol **21:** 30–36

Giehl RFH, Lima JE, von Wirén N (2012) Localized iron supply triggers lateral root elongation in *Arabidopsis* by altering the AUX1-mediated auxin distribution. Plant Cell **24:** 33–49

Giehl RFH, von Wirén N (2014) Root nutrient foraging. Plant Physiol **166:** 509–517

Gifford ML, Dean A, Gutierrez RA, Coruzzi GM, Birnbaum KD (2008) Cell-specific nitrogen responses mediate developmental plasticity. Proc Natl Acad Sci USA **105:** 803–808

Gruber BD, Giehl RFH, Friedel S, von Wirén N (2013) Plasticity of the Arabidopsis root system under nutrient deficiencies. Plant Physiol **163:** 161–179

Guan P, Wang R, Nacry P, Breton G, Kay SA, Pruneda-Paz JL, Davani A, Crawford NM (2014) Nitrate foraging by *Arabidopsis* roots is mediated by the transcription factor TCP20 through the systemic signaling pathway. Proc Natl Acad Sci USA **111:** 15267–15272

Horton MW, Hancock AM, Huang YS, Toomajian C, Atwell S, Auton A, Muliyati NW, Platt A, Sperone FG, Vilhjálmsson BJ, et al (2012) Genome-wide patterns of genetic variation in worldwide *Arabidopsis thaliana* accessions from the RegMap panel. Nat Genet **44:** 212–216

Hossain Z, McGarvey B, Amyot L, Gruber M, Jung J, Hannoufa A (2012) *DIMINUTO 1* affects the lignin profile and secondary cell wall formation in Arabidopsis. Planta **235:** 485–498

Jia Z, von Wirén N (2020) Signaling pathways underlying nitrogen-dependent changes in root system architecture: From model to crop species. J Exp Bot eraa033, doi:10.1093/jxb/eraa033

Jia Z, Giehl RFH, Meyer RC, Altmann T, von Wirén N (2019) Natural variation of BSK3 tunes brassinosteroid signaling to regulate root foraging under low nitrogen. Nat Commun **10:** 2378

Kang HMZ, Zaitlen NA, Wade CM, Kirby A, Heckerman D, Daly MJ, Eskin E (2008) Efficient control of population structure in model organism association mapping. Genetics **178:** 1709–1723

Kellermeier F, Armengaud P, Seditas TJ, Danku J, Salt DE, Amtmann A (2014) Analysis of the root system architecture of *Arabidopsis* provides a quantitative readout of crosstalk between nutritional signals. Plant Cell **26:** 1480–1496

Klahre U, Noguchi T, Fujioka S, Takatsuto S, Yokota T, Nomura T, Yoshida S, Chua NH (1998) The *Arabidopsis DIMINUTO/DWARF1* gene encodes a protein involved in steroid synthesis. Plant Cell **10:** 1677–1690

Kochian LV, Piñeros MA, Liu J, Magalhaes JV (2015) Plant adaptation to acid soils: The molecular basis for crop aluminum resistance. Annu Rev Plant Biol **66:** 571–598

Kooke R, Kruijer W, Bours R, Becker F, Kuhn A, van de Geest H, Buntjer J, Doeswijk T, Guerra J, Bouwmeester H, et al (2016) Genome-wide association mapping and genomic prediction elucidate the genetic architecture of morphological traits in Arabidopsis. Plant Physiol **170:** 2187–2203

Krouk G, Lacombe B, Bielach A, Perrine-Walker F, Malinska K, Mounier E, Hoyerova K, Tillard P, Leon S, Ljung K, et al (2010) Nitrate-regulated auxin transport by NRT1.1 defines a mechanism for nutrient sensing in plants. Dev Cell **18:** 927–937

Lima JE, Kojima S, Takahashi H, von Wirén N (2010) Ammonium triggers lateral root branching in *Arabidopsis* in an AMMONIUM TRANSPORTER1; 3-dependent manner. Plant Cell **22:** 3621–3633

Liu Y, von Wirén N (2017) Ammonium as a signal for physiological and morphological responses in plants. J Exp Bot **68:** 2581–2592

Liu Y, Jia Z, Li X, Wang Z, Chen F, Mi G, Forde B, Takahashi H, Yuan L (2020) Involvement of a truncated MADS-box transcription factor ZmTMM1 in root nitrate foraging. J Exp Bot eraa116, doi:10.1093/jxb/eraa116

Liu Y, Lai N, Gao K, Chen F, Yuan L, Mi G (2013) Ammonium inhibits primary root growth by reducing the length of meristem and elongation zone and decreasing elemental expansion rate in the root apex in *Arabidopsis thaliana*. PLoS One **8:** e61031

Ma W, Li J, Qu B, He X, Zhao X, Li B, Fu X, Tong Y (2014) Auxin biosynthetic gene TAR2 is involved in low nitrogen-mediated reprogramming of root architecture in Arabidopsis. Plant J **78:** 70–79

Martins S, Montiel-Jorda A, Cayrel A, Huguet S, Roux CP, Ljung K, Vert G (2017) Brassinosteroid signaling-dependent root responses to prolonged elevated ambient temperature. Nat Commun **8:** 309

Mounier E, Pervent M, Ljung K, Gojon A, Nacry P (2014) Auxin-mediated nitrate signalling by NRT1.1 participates in the adaptive response of *Arabidopsis* root architecture to the spatial heterogeneity of nitrate availability. Plant Cell Environ **37:** 162–174

Müller J, Toev T, Heisters M, Teller J, Moore KL, Hause G, Dinesh DC, Bürstenbinder K, Abel S (2015) Iron-dependent callose deposition adjusts root meristem maintenance to phosphate availability. Dev Cell **33:** 216–230

Pérez-Torres CA, López-Bucio J, Cruz-Ramírez A, Ibarra-Laclette E, Dharmasiri S, Estelle M, Herrera-Estrella L (2008) Phosphate availability alters lateral root development in *Arabidopsis* by modulating auxin sensitivity via a mechanism involving the TIR1 auxin receptor. Plant Cell **20:** 3258–3272

Pfaffl MW (2001) A new mathematical model for relative quantification in real-time RT-PCR. Nucleic Acids Res **29:** e45

Qin L, Walk TC, Han P, Chen L, Zhang S, Li Y, Hu X, Xie L, Yang Y, Liu J, et al (2019) Adaption of roots to nitrogen deficiency revealed by 3D quantification and proteomic analysis. Plant Physiol **179:** 329–347

Remans T, Nacry P, Pervent M, Filleur S, Diatloff E, Mounier E, Tillard P, Forde BG, Gojon A (2006) The Arabidopsis NRT1.1 transporter participates in the signaling pathway triggering root colonization of nitrate-rich patches. Proc Natl Acad Sci USA **103:** 19206–19211

Ristova D, Carré C, Pervent M, Medici A, Kim GJ, Scalia D, Ruffel S, Birnbaum KD, Lacombe B, Busch W, et al (2016) Combinatorial interaction network of transcriptomic and phenotypic responses to nitrogen and hormones in the *Arabidopsis thaliana* root. Sci Signal **9:** rs13

R Core Team (2013) R: A Language and Environment for Statistical Computing. The R Foundation for Statistical Computing, Vienna

Satbhai SB, Setzer C, Freynschlag F, Slovak R, Kerdaffrec E, Busch W (2017) Natural allelic variation of *FRO2* modulates *Arabidopsis* root growth under iron deficiency. Nat Commun **8:** 15603

Schluter U, Kopke D, Altmann T, Mussig C (2002) Analysis of carbohydrate metabolism of *CPD* antisense plants and the brassinosteroid-deficient *cbb1* mutant. Plant Cell Environ **25:** 783–791

Schmid NB, Giehl RFH, Döll S, Mock H-P, Strehmel N, Scheel D, Kong X, Hider RC, von Wirén N (2014) Feruloyl-CoA 6′-Hydroxylase1-dependent coumarins mediate iron acquisition from alkaline substrates in Arabidopsis. Plant Physiol **164:** 160–72

Shao A, Ma W, Zhao X, Hu M, He X, Teng W, Li H, Tong Y (2017) The auxin biosynthetic *TRYPTOPHAN AMINOTRANSFERASE RELATED TaTAR2.1-3A* increases grain yield of wheat. Plant Physiol **174:** 2274–2288

Singh AP, Fridman Y, Friedlander-Shani L, Tarkowska D, Strnad M, Savaldi-Goldstein S (2014) Activity of the brassinosteroid transcription factors BRASSINAZOLE RESISTANT1 and BRASSINOSTEROID INSENSITIVE1-ETHYL METHANESULFONATE-SUPPRESSOR1/BRASSINAZOLE RESISTANT2 blocks developmental reprogramming in response to low phosphate availability. Plant Physiol **166:** 678–688

Singh AP, Fridman Y, Holland N, Ackerman-Lavert M, Zananiri R, Jaillais Y, Henn A, Savaldi-Goldstein S (2018) Interdependent nutrient availability and steroid hormone signals facilitate root growth plasticity. Dev Cell **46:** 59–72

Sun J, Xu Y, Ye S, Jiang H, Chen Q, Liu F, Zhou W, Chen R, Li X, Tietz O, et al (2009) Arabidopsis ASA1 is important for jasmonate-mediated regulation of auxin biosynthesis and transport during lateral root formation. Plant Cell **21:** 1495–1511

Takahashi T, Gasch A, Nishizawa N, Chua NH (1995) The *DIMINUTO* gene of Arabidopsis is involved in regulating cell elongation. Genes Dev **9:** 97–107

Vidal EA, Araus V, Lu C, Parry G, Green PJ, Coruzzi GM, Gutiérrez RA (2010) Nitrate-responsive miR393/AFB3 regulatory module controls root system architecture in *Arabidopsis thaliana*. Proc Natl Acad Sci USA **107:** 4477–4482

Wang YY, Hsu PK, Tsay YF (2012a) Uptake, allocation and signaling of nitrate. Trends Plant Sci **17:** 458–467

Wang ZY, Bai MY, Oh E, Zhu JY (2012b) Brassinosteroid signaling network and regulation of photomorphogenesis. Annu Rev Genet **46:** 701–724

Yang J, Suzuki M, McCarty DR (2016) Essential role of conserved DUF177A protein in plastid 23S rRNA accumulation and plant embryogenesis. J Exp Bot **67:** 5447–5460

Youn JH, Kim TW, Joo SH, Son SH, Roh J, Kim S, Kim TW, Kim SK (2018) Function and molecular regulation of DWARF1 as a C-24 reductase in brassinosteroid biosynthesis in Arabidopsis. J Exp Bot **69:** 1873–1886

Yuan L, Loqué D, Kojima S, Rauch S, Ishiyama K, Inoue E, Takahashi H, von Wirén N (2007) The organization of high-affinity ammonium uptake in *Arabidopsis* roots depends on the spatial arrangement and biochemical properties of AMT1-type transporters. Plant Cell **19:** 2636–2652

Zhang H, Forde BG (1998) An *Arabidopsis* MADS box gene that controls nutrient-induced changes in root architecture. Science **279:** 407–409